Electronic Supplementary Information (ESI)

Sequential separation of cerium (Ce) and neodymium (Nd) in geological samples for high-precision analysis of stable Ce isotopes, stable and radiogenic Nd isotopes by MC-ICP-MS

Weiming Ding, Xin-Yuan Zheng*

Department of Earth and Environmental Sciences, University of Minnesota-Twin Cities, Minneapolis, MN 55455, USA

Email: zhengxy@umn.edu

α-HIBA reagent preparation

~200 g α-HIBA powder (Aldrich 99%, cat. No. 323594-100G) was dissolved in ~1.92 L Milli-Q water (18.2 MΩ · cm) to make ~1 M α-HIBA stock solution. The accurate molarity of the solution was titrated to be 0.955 M using 1 N NaOH standard solution. The unpurified 0.955 M α-HIBA stock solution was measured on Thermo iCAP^{TM} TQ-ICP-MS and determined to have a Ce concentration of 52.5 pg/mL. The stock α-HIBA solution was then purified through 3 Bio-Rad columns (20 mL resin bed) positioned in a tandem fashion. Each column was filled with precleaned Bio-Rad AG50W-X8 resin (H^+ form, 200-400 mesh) to remove lanthanides and other cation impurities from the α-HIBA solution. After chromatographic purification, the α-HIBA solution was titrated again, and the result (i.e., 0.956 M) indicated quantitative recovery of α-HIBA. Based on our measurements on TQ-ICP-MS, the purified α-HIBA stock solution had a Ce concentration of 0.6 pg/mL. The volume of the purified α-HIBA solution was determined to be 1860 mL using an acid-cleaned measuring cylinder. 235 mL of 9 M Optima^{TM} ammonia solution was added into the α-HIBA solution gradually to adjust its pH to 4.68±0.02 at room temperature, leaving the total volume of α-HIBA solution as 2.095 L. Pre-cleaned pencil-thin epoxy body gel-filled combination electrode (FisherbrandTM, Cat. No. 13-620-290) coupled with accumet™ AP125 portable pH/Ion/mV/Temperature meter (Fisherbrand™, Cat. No. 13-636-AP125A) was used to monitor the pH variations. Therefore, the concentration of pH-adjusted α-HIBA solution could be calculated to be 0.849 M. The final 0.150 M and 0.225 M α-HIBA solutions used in our chromatographic separation procedure were then prepared gravimetrically by diluting the 0.849 M α-HIBA solution (density = 1.027 g/mL) with Milli-Q water. Because α-HIBA is a weak acid that does not disassociate completely in aqueous solution, a mixture of α-HIBA and ammonium solution essentially acts a buffer system. Thus, the pH of the α-HIBA solution remained nearly constant during dilution by water.

Converting AG50W-X4 resin from H^+ to NH_4^+ form

~500 g precleaned Bio-Rad AG50W-X4 resin (200-400 mesh) was loaded into a Nalgene^{TM} Polypropylene separation funnel and washed with Milli-Q water until pH of the eluate became neutral. The resin was then

washed with ~9 M Optima^{TM} ammonia solution until the pH of eluate had the same pH (i.e., 12.77) of the ~9 M ammonia solution added into the funnel. Once the pH of the eluate no longer changed and the resin was fully converted to the NH_4^+ form, Milli-Q water was added into the funnel to bring the pH of eluate back to neutral. Finally, the resin was equilibrated with 0.150 M α-HIBA solution, and then transferred and stored in a clean FEP bottle in dark.

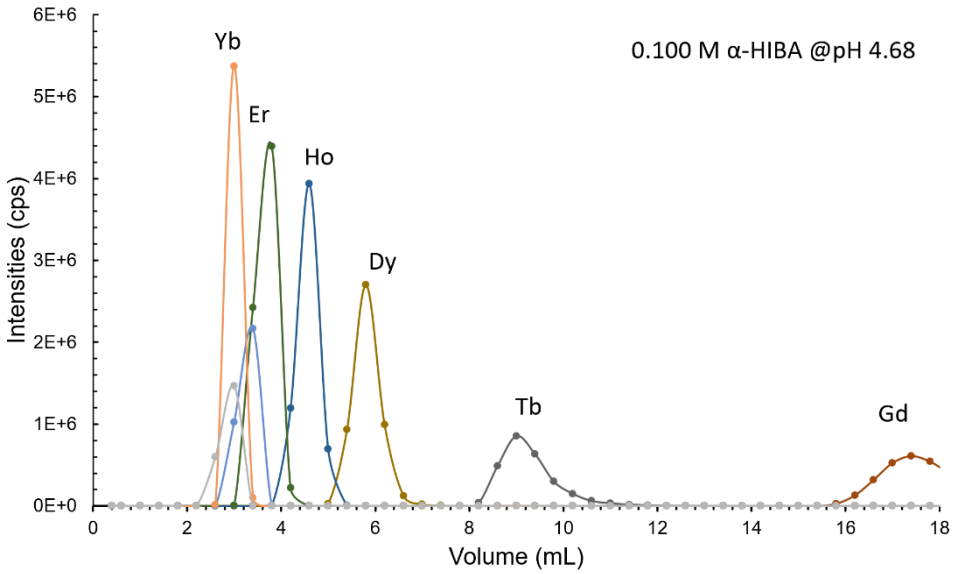

Fig. S1 Elution curve of the α-HIBA column using 0.100 M α-HIBA (pH = 4.68) as an eluent. Bio-Rad AG50W-X4 resin (NH_4^+ form, 200-400 mesh) was stored in 0.150 M α-HIBA prior to use. An in-house high-purity multi-REE solution was used as a sample and loaded to column in 0.4 mL of 0.1 M HCl, washed with 0.2 mL Milli-Q water and subsequently with 0.100 M α-HIBA solution.

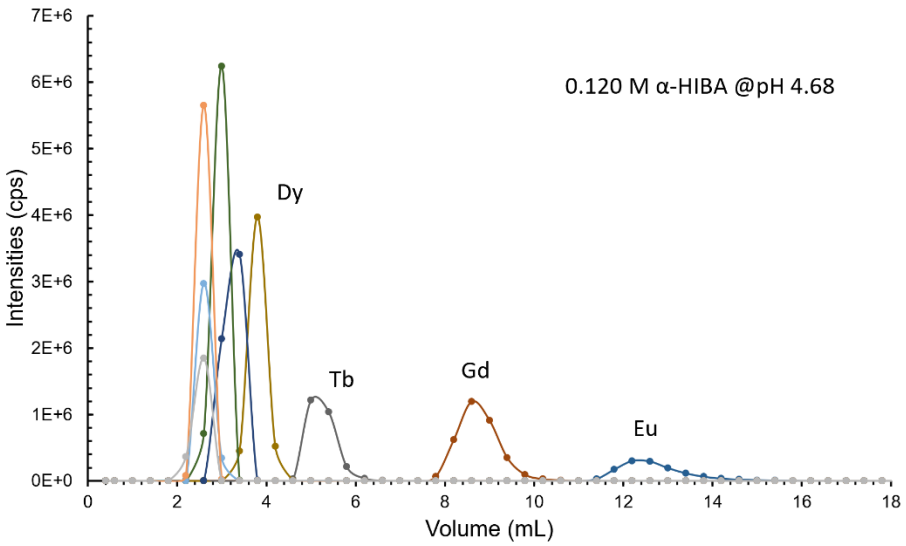

Fig. S2 Elution curve of the α-HIBA column using 0.120 M α-HIBA (pH = 4.68) as an eluent. Bio-Rad AG50W-X4 resin (NH_4^+ form, 200-400 mesh) was stored in 0.150 M α-HIBA prior to use. An in-house high-purity multi-REE solution was used as a sample and loaded to column in 0.4 mL of 0.1 M HCl, washed with 0.2 mL Milli-Q water and subsequently with 0.120 M α-HIBA solution.

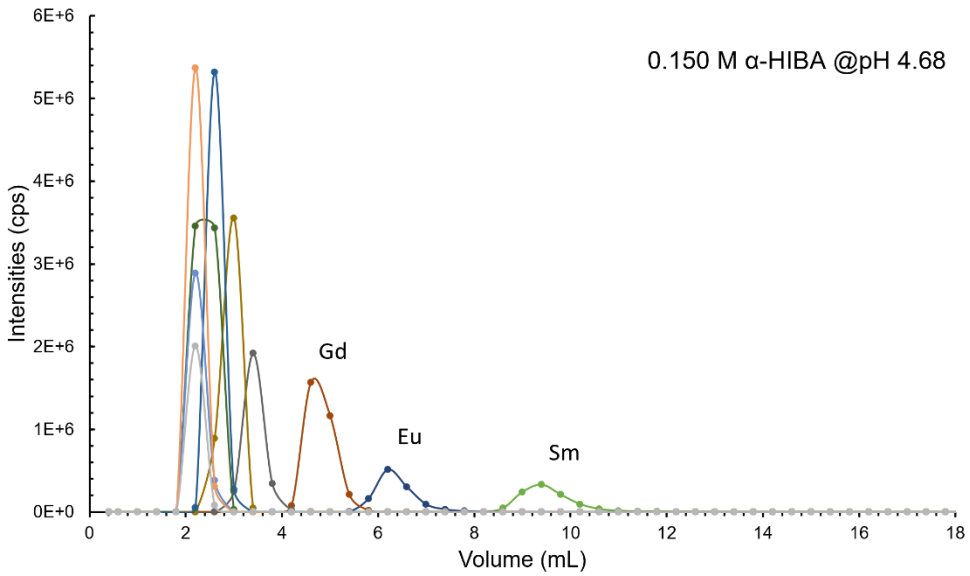

Fig. S3 Elution curve of the α-HIBA column using 0.150 M α-HIBA (pH = 4.68) as an eluent. Bio-Rad AG50W-X4 resin (NH_4^+ form, 200-400 mesh) was stored in 0.150 M α-HIBA prior to use. An in-house high-purity multi-REE solution was used as a sample and loaded to column in 0.4 mL of 0.1 M HCl, washed with 0.2 mL Milli-Q water and subsequently with 0.150 M α-HIBA solution.

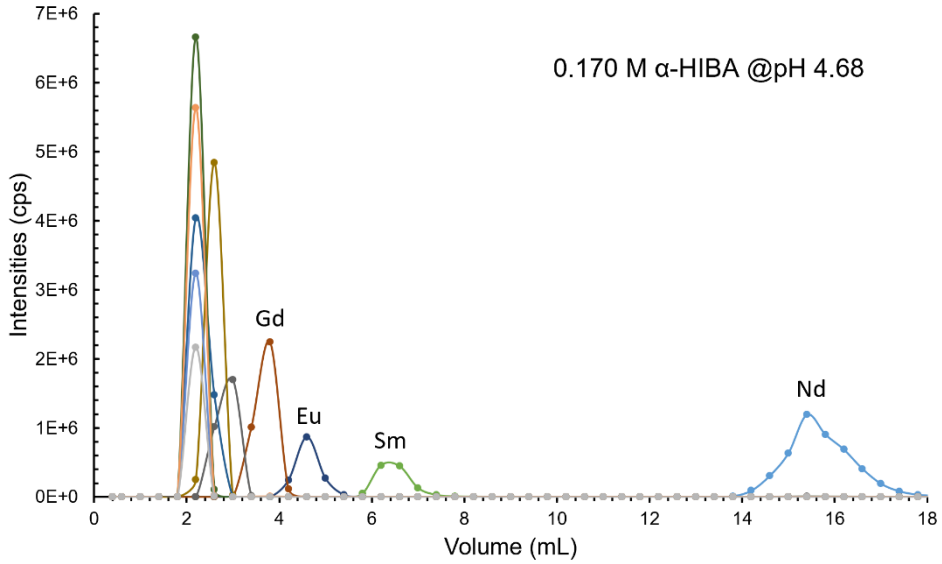

Fig. S4 Elution curve of the α-HIBA column using 0.170 M α-HIBA (pH = 4.68) as an eluent. Bio-Rad AG50W-X4 resin (NH_4^+ form, 200-400 mesh) was stored in 0.150 M α-HIBA prior to use. An in-house high-purity multi-REE solution was used as a sample and loaded to column in 0.4 mL of 0.1 M HCl, washed with 0.2 mL Milli-Q water and subsequently with 0.170 M α-HIBA solution.

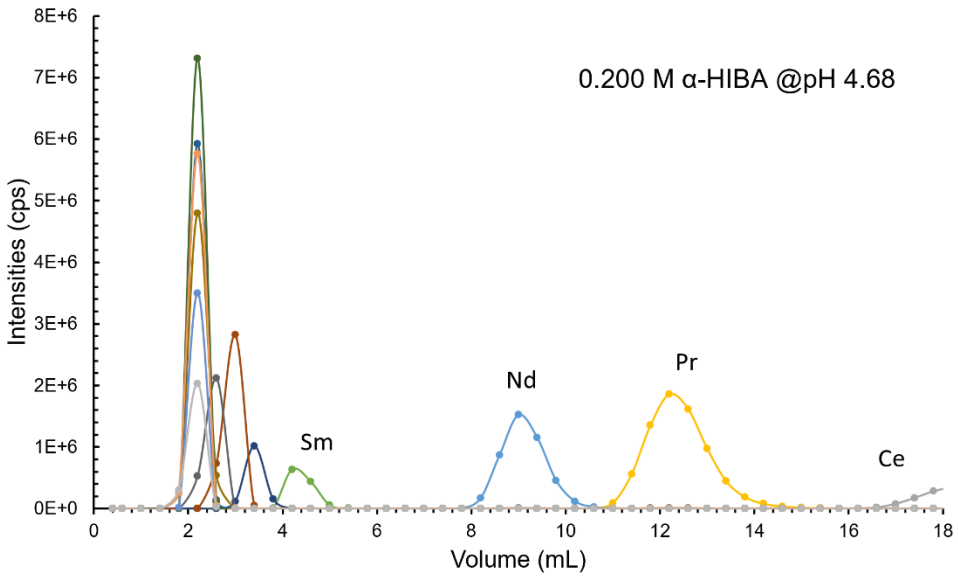

Fig. S5 Elution curve of the α-HIBA column using 0.200 M α-HIBA (pH = 4.68) as an eluent. Bio-Rad AG50W-X4 resin (NH_4^+ form, 200-400 mesh) was stored in 0.150 M α-HIBA prior to use. An in-house high-purity multi-REE solution was used as a sample and loaded to column in 0.4 mL of 0.1 M HCl, washed with 0.2 mL Milli-Q water and subsequently with 0.200 M α-HIBA solution.

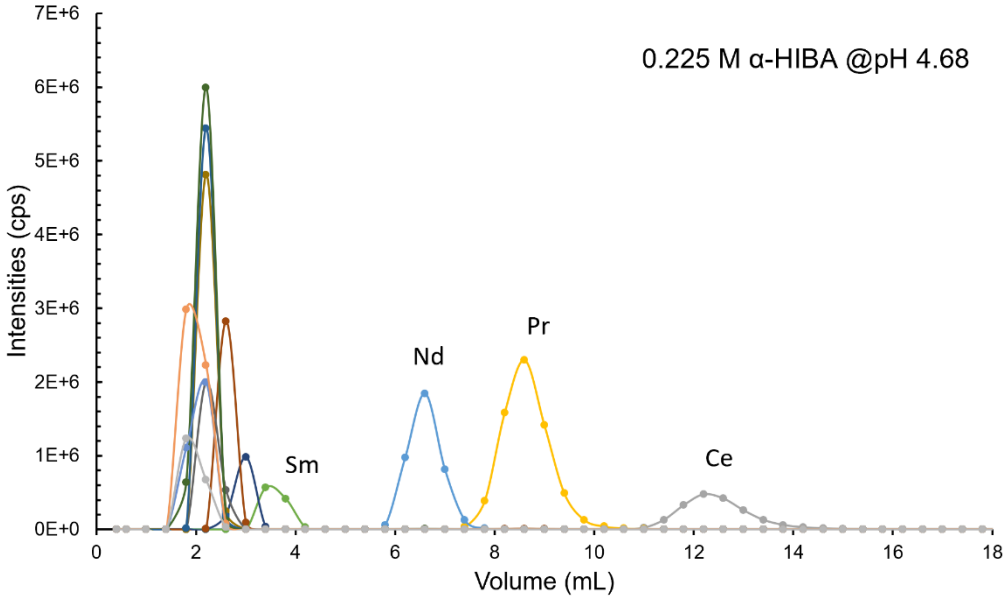

Fig. S6 Elution curve of the α-HIBA column using 0.225 M α-HIBA (pH = 4.68) as an eluent. Bio-Rad AG50W-X4 resin (NH_4^+ form, 200-400 mesh) was stored in 0.150 M α-HIBA prior to use. An in-house high-purity multi-REE solution was used as a sample and loaded to column in 0.4 mL of 0.1 M HCl, washed with 0.2 mL Milli-Q water and subsequently with 0.225 M α-HIBA solution.

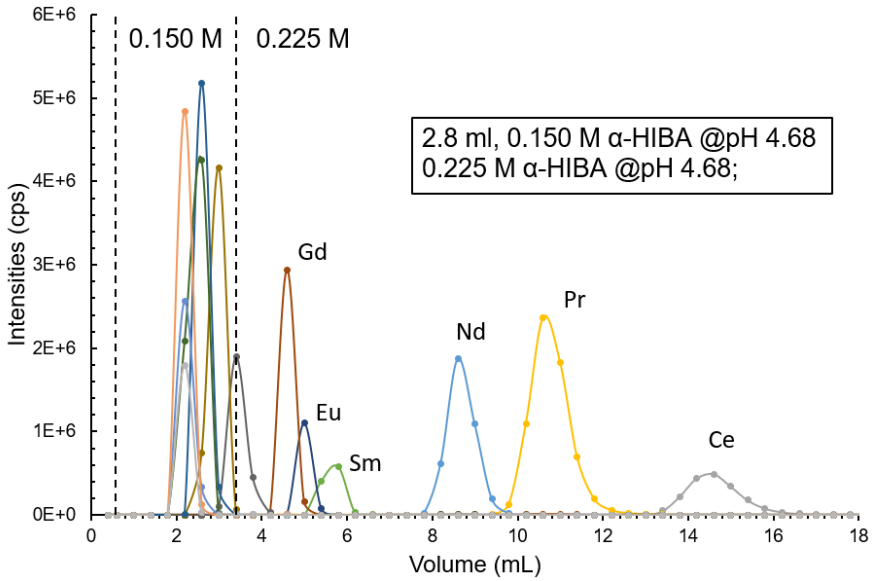

Fig. S7 Elution curve of the α-HIBA column using 0.150 M + 0.225 M α-HIBA (pH = 4.68) as an eluent. Bio-Rad AG50W-X4 resin (NH_4^+ form, 200-400 mesh) was stored in 0.150 M α-HIBA prior to use. An in-house high-purity multi-REE solution was used as a sample and loaded to column in 0.4 mL of 0.1 M HCl, washed with 0.2 mL Milli-Q water and subsequently with 2.8 mL 0.150 M α-HIBA and finally with 0.225 M α-HIBA solution. This elution procedure was adopted for sequential Ce and Nd separations in geological reference materials in our study.

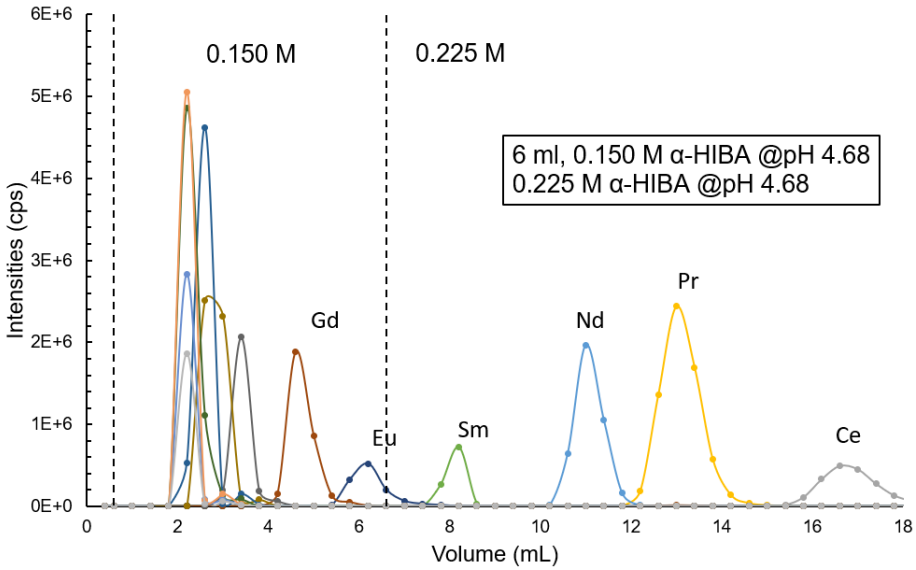

Fig. S8 Elution curve of the α-HIBA column using 0.150 M + 0.225 M α-HIBA (pH = 4.68) as an eluent. Bio-Rad AG50W-X4 resin (NH_4^+ form, 200-400 mesh) was stored in 0.150 M α-HIBA prior to use. An in-house high-purity multi-REE solution was used as a sample and loaded to column in 0.4 mL of 0.1 M HCl, washed with 0.2 mL Milli-Q water and subsequently with 6 mL 0.150 M α-HIBA and finally with 0.225 M α-HIBA solution.

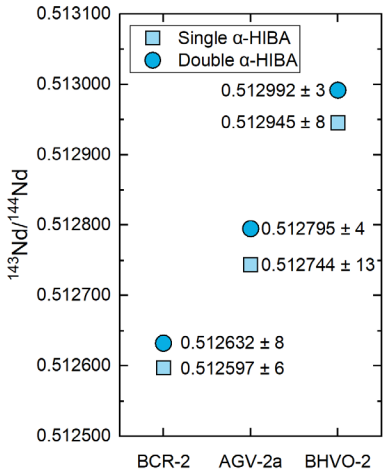

Fig. S9 Radiogenic $^{143}Nd/^{144}Nd$ measurements of BCR-2, AGV-2a and BHVO-2 processed through the α-HIBA column, eluted by either 0.225 M solution (labeled as "single α-HIBA" in the plot, light blue squares) or 0.150 M + 0.225 M α-HIBA solution (labeled as "double α-HIBA" in the plot, dark blue circles). Samples prepared by single molarity α-HIBA elution showed large isotopic deviations from recommended values because of the presence of high level of Sm that interferes with Nd isotope analysis on MC-ICP-MS. In contrast, elution with a combination of 0.150 M and 0.225 M α-HIBA provided significantly better Sm and Nd separation, and, thus, accurate $^{143}Nd/^{144}Nd$ ratios were acquired for all three reference materials. (Recommended $^{143}Nd/^{144}Nd$ is 0.512638 for BCR-2, 0.512790 for AGV-2a, and 0.512990 for BHVO-2)[1].

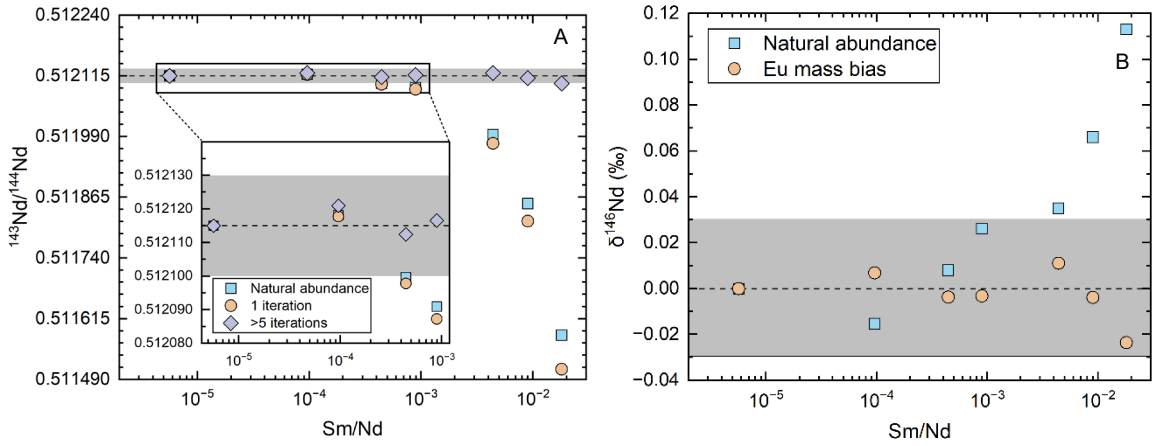

Fig. S10 (A) Comparison of Sm isobaric correction methods for radiogenic $^{143}Nd/^{144}Nd$ analyses. JNdi-1 was used as the pure Nd solutions. Blue squares represent corrected results when an average natural $^{144}Sm/^{147}Sm$ ratio was used to calculate isobaric ^{144}Sm interferences from the measured ^{147}Sm intensities without considering instrumental mass bias. Orange circles represent 1 iteration correction when the average natural $^{144}Sm/^{147}Sm$ ratio was taken as an initial input but then adjusted for instrumental mass bias based on normalization of the measured $^{146}Nd/^{144}Nd$ ratios to 0.7219 by an exponential law. Purple diamonds signify correction results after >5 iterations. The iterative correction method allows for correction of Sm isobaric interferences up to Sm/Nd mass ratios of ~0.01. (B) Comparison of Sm isobaric correction methods for stable Nd isotope analyses. Multiple iteration corrections cannot be applied because Sm only has isobaric interferences on Nd but does not interfere on Eu. However, correction of Sm isobaric interferences that considers instrumental mass bias is still superior to the correction that does not consider instrumental mass bias.

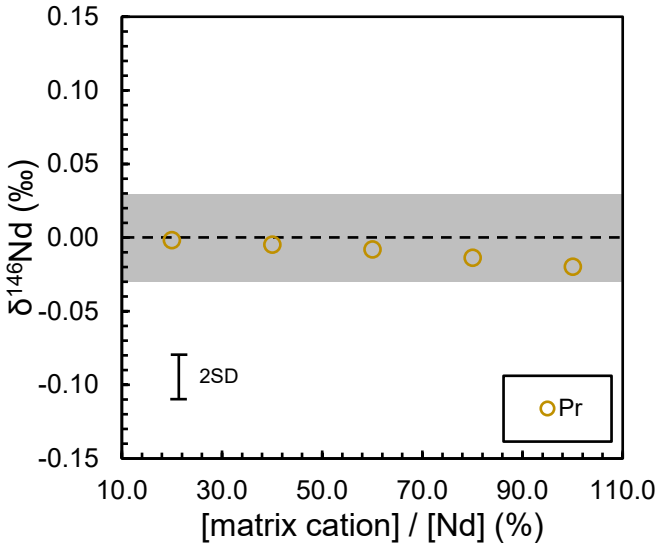

Fig. S11 Testing of Pr matrix effect on stable Nd isotope measurement. It is found that a Pr/Nd mass ratio of up to 100% has no resolvable impact on stable Nd isotope analysis.

Table S1 Comparison of stable Ce and Nd isotope analytical methodologies

				Ce					Nd					
Chromatographic method	**Instrument**	**Plasma condition[a]**	**DS / TS needed[b]**	**Yield**	**Nd/Ce in Ce cut[c]**	**Blank (pg)**	**Oxide ratio[d]**	**2SD[e] (‰)**	**Yield**	**Ce/Nd in Nd cut[c]**	**Sm/Nd in Nd cut[c]**	**Blank (pg)**	**2SD[e] (‰)**	**References**
Ce only														
AG50W-X8 + LN resins (BrO_3^- + H_2O_2)	Neptune MC-ICP-MS	Wet plasma		>99%	~0.65%	<10	1.5-8%	0.024-0.064	-	-	-	-	-	Nakada et al. (2013, 2016, 2017)[2-4]
	Nu HR MC-ICP-MS	Dry plasma (Nu DSN + Aridus I)		-	-	-	-	0.02-0.07	-	-	-	-	-	Laycock et al. (2016)[5]
AG50W-X8 + LN resins (BrO_3^- + H_2O_2)	Neptune MC-ICP-MS	Dry plasma (Aridus II)		>99%	-	-	0.01%	0.025-0.043	-	-	-	-	-	Nakada et al. (2019)[6]
AG50W-X8 + LN resins (BrO_3^- + H_2O_2)	Triton Plus TIMS		TS	-	0.1%	500	<0.2%	0.028-0.099	-	-	-	-	-	Bonnand et al. (2019)[7]
AG1-X8 + AG50W-X8 + LN resins(BrO_3^- + H_2O_2)	HR Nu Plasma II MC-ICPMS	Dry plasma (Aridus II)		-	-	-	-	0.03-0.19	-	-	-	-	-	Pourkhorsandi et al. (2021)[8]
DGA resin	Neptune Plus MC-ICP-MS	Wet plasma		>99.5%	<0.03%	170-200	<2%	0.013-0.049	-	-	-	-	-	Liu et al. (2021, 2023a)[9, 10]
Nd only														
AG50W-X8 resin (α-HIBA)	VG Sector 54-30 TIMS		DS	-	-	-	-	-	98.8%	-	-	-	0.01-0.036	Wakaki and Tanaka (2012)[11]
AG50W-X12 + LN resins	Neptune Plus MC-ICP-MS	Wet plasma		-	-	-	-	-	>96%	<0.5%	-	-	0.014-0.054	Ma et al. (2013)[12]
AG50W-X8 + LN resins (BrO_3^-)	Neptune Plus MC-ICP-MS	Dry plasma (Apex IR)		-	-	-	-	-	>99.5%	<0.0012%	<0.0015%	<100	0.006-0.028	Saji et al. (2016)[13]
DGA resin	Nu Plasma II MC-ICP-MS	Dry plasma (Aridus II)		-	-	-	-	-	>98.7%	<0.7%		30-70	0.029-0.033	Wang et al. (2017)[14]
AG50W-X8 + LN resins	Triton Plus TIMS		DS	-	-	-	-	-	>96.5%	<5%	-	3-55	<0.017	McCoy-West et al. (2017, 2020)[15, 16]
DGA resin	Neptune Plus MC-ICP-MS	Wet plasma		-	-	-	-	-	>99%	<0.3%	-	20-310	0.011-0.042	Bai et al. (2021, 2022b)[17, 18]
DGA resin	Triton XT TIMS		DS	-	-	-	-	-	>99%	-	-	<50	0.016	Liu et al. (2023b)[19]

Both Ce and Nd (sequential)														
AG50W-X8 + TRU + LN resins	Nu plasma 500 MC-ICP-MS	Dry plasma (Aridus)		98%	0.01-0.1%	<1,000	-	0.02-0.10	99%	-	-	<1,000	0.02-0.06	Ohno and Hirata (2013)[20]
AG50W-X12 + DGA resins	Neptune Plus MC-ICP-MS	Wet plasma		99.3%	0.005-0.028%	48	<2%	0.034-0.046	99.5%	0.023-0.084%	-	33	0.018-0.032	Bai et al. (2022a)[21]
DGA + LN resins (FPLC system)	Neptune Plus MC-ICP-MS	Dry plasma (Apex Q+ Spiro TMD, Apex Omega, Aridus I)	DS	>95% (2021) 40-70% (2023)	-	<250	-	<0.1[f] 0.08-0.036	>95% (2021) 40-70% (2023)	-	-	<250	<0.1[f] 0.022-0.044	Hu et al. (2021, 2023)[22, 23]
AG50W-X8 + AG50W-X4 (α-HIBA) + DGA resins	Nu "Sapphire" MC-ICP-MS	Dry plasma (Apex Omega HF)		>99%	0.006-0.03%	46	<0.05%	0.009-0.051	>99%	-	<0.02%	2	0.01-0.042	This study

[a] only applicable to MC-ICP-MS.

[b] DS represents double spike, TS represents triple spike.

[c] Nd/Ce in Ce cut indicates total Nd/Ce mass ratios in the pure Ce cuts after chromatographic chemistry, Ce/Nd and Sm/Nd in Nd cut indicates total Ce/Nd and Sm/Nd mass ratios in the pure Nd cuts after chromatographic chemistry.

[d] Oxide ratio signifies $^{140}Ce^{16}O^{+}/^{140}Ce^{+}$ intensity ratios during the measurements.

[e] 2SD for Ce is 2 standard deviations of $\delta^{142}Ce$, 2SD for Nd is 2 standard deviations of $\delta^{146}Nd$.

[f] Such precisions are from Hu et al. (2021)[23] with no double spike addition.

Table S2 Stable Nd isotope compositions in different Nd fractions from α-HIBA chromatographic chemistry. The initial loading mass of Nd is 501.9 ng, yielding 99% recovery rate.

Sample ID	Nd mass (ng)	Percentage of Nd	δ^{145}Nd (‰)	δ^{146}Nd (‰)	δ^{148}Nd (‰)	δ^{150}Nd (‰)
Fract 1	68.40	13.80%	0.309	0.587	1.167	1.728
Fract 2	157.55	31.78%	0.108	0.217	0.446	0.640
Fract 3	85.85	17.32%	0.009	-0.018	0.001	-0.044
Fract 4	34.91	7.04%	-0.086	-0.131	-0.233	-0.390
Fract 5	77.36	15.60%	-0.129	-0.271	-0.518	-0.830
Fract 6	71.70	14.46%	-0.256	-0.498	-1.000	-1.451
Bulk	495.76		0.015	0.023	0.061	0.067

Table S3 Stable Ce isotope compositions in different Ce fractions from α-HIBA chromatographic chemistry. The initial loading mass of Ce is 495.3 ng, yielding 100% recovery rate.

Sample ID	Ce mass (ng)	Percentage of Ce	δ^{142}Ce (‰)
Fract 1	304.88	61.23%	0.149
Fract 2	85.36	17.14%	-0.211
Fract 3	54.27	10.90%	-0.290
Fract 4	19.51	3.92%	-0.498
Fract 5	12.50	2.51%	-0.418
Fract 6	10.97	2.20%	-0.636
Fract 7	4.88	0.98%	-0.846
Fract 8	5.55	1.11%	
Bulk	497.93		-0.029

Table S4 A compilation of stable Ce isotope values for reference materials analyzed in this study[a].

Sample Name	Description	$\delta^{142}Ce_{NIST3110}$ (‰)	2SD	N[b]	References (Note)
UMN Ce I	$Ce_2(CO_3)_3$	0.126	0.020	18	(Direct analyses)
		0.120		1	(After purification)
		0.126	0.020	19	**This study**
UMN Ce II	$Ce(NO_3)_3$	0.007	0.017	8	(Direct analyses)
		0.024		1	(After purification)
		0.009	0.020	9	**This study**
UMN Ce III	$CeCl_3$	0.104	0.015	4	(Direct analyses)
		0.109		1	(After purification)
		0.105	0.014	5	**This study**
BCR-2	Basalt	0.037	0.029	3	**This study**
		0.010	0.037	3*	Bai et al., 2022a[21]
		0.006		1*	Bai et al., 2022a[21]
		0.032	0.024	3*	Liu et al., 2021[9]
		0.012	0.022	3*	Liu et al., 2021[9]
		0.052	0.032	3	Nakada et al., 2019[6]
mean		***0.025***	***0.033***		***interlaboratory***
BHVO-2	Basalt	0.006	0.037	3	**This study**
		0.032	0.036	1[DS]	Hu et al., 2023[c 22]
		0.058	0.008	1[DS]	Hu et al., 2023[22]
		-0.019	0.036	4*	Liu et al., 2023a[10]
		-0.054	0.043	1	Li et al., 2023a, b[24, 25]
		0.000	0.046	3*	Bai et al., 2022a[21]
		0.004	0.040	3	Nakada et al., 2019[6]
mean		***0.004***	***0.066***		***interlaboratory***
COQ-1	Carbonatite	0.025	0.048	3	**This study**
		-0.027	0.020	5*	Liu et al., 2021[9]
		-0.003	0.039	5*	Liu et al., 2021[9]
		0.042	0.028	3	Nakada et al., 2019[6]
mean		***0.009***	***0.053***		***interlaboratory***
AGV-2/AGV-2a	Andesite	0.022	0.025	3	**This study**
		0.032	0.022	1[DS]	Hu et al., 2023[22]
		0.036	0.014	1[DS]	Hu et al., 2023[22]
		-0.018	0.042	3*	Bai et al., 2022a[21]
		-0.024	0.040	3*	Liu et al., 2021[9]
		-0.009	0.028	3	Nakada et al., 2019[6]
mean		***0.006***	***0.049***		***interlaboratory***
GSP-2	Granodiorite	-0.002	0.051	3	**This study**
		-0.057	0.034	1	Li et al., 2023a, b[24, 25]

		0.022	0.035	3*	Bai et al., 2022a[21]
		-0.023	0.024	3*	Liu et al., 2021[9]
		-0.027	0.049	3*	Liu et al., 2021[9]
mean		***-0.017***	***0.053***		***interlaboratory***
SDC-1	Mica Schist	0.031	0.009	2	**This study**
		-0.022	0.032	1[DS]	Hu et al., 2023[22]
JMn-1	Mn nodule	0.095	0.010	3	**This study**
		0.110	0.025	3	Nakada et al., 2019[6]
		0.104	0.034	1	Nakada et al., 2016[3]
		0.050	0.100	1	Ohno & Hirata, 2013[20]
mean		***0.090***	***0.047***		***interlaboratory***
NOD-P-1	Mn nodule	0.112		1	**This study**
		0.175	0.045	4*	Liu et al., 2023a[10]
		0.180	0.024	3*	Liu et al., 2023a[10]
		0.168	0.040	4*	Liu et al., 2023a[10]
		0.176	0.031	4*	Liu et al., 2023a[10]
		0.112	0.046	3*	Bai et al., 2022a[21]
mean		***0.154***	***0.060***		***interlaboratory***
NOD-A-1	Mn nodule	0.126		1	**This study**
		0.132	0.020	1[DS]	Hu et al., 2023[22]
		0.115	0.021	4*	Liu et al., 2023a[10]
		0.118	0.036	4*	Liu et al., 2023a[10]
		0.104	0.022	5*	Liu et al., 2023a[10]
		0.105	0.038	4*	Liu et al., 2023a[10]
		0.117	0.043	1	Li et al., 2023a, b[24, 25]
		0.131	0.042	3*	Bai et al., 2022a[21]
mean		***0.119***	***0.020***		***interlaboratory***

[a] Data from Pourkhorsandi et al., 2021[8] is not included in this compilation because their data were reported against an Ames Ce reference solution, and the conversion of their standard to NIST 3110 Ce solution is unknown.

[b] N is the number of individual replicate analyses, processed independently through chromatographic purification, and each value is comprised of at least 3 repeated measurements in the same solution; * indicates the number of sample-standard bracketing measurements for the same solution; [DS] indicates the double spike technique.

[c] Since Hu et al., 2023[22] used OL-REE as the bracketing standard instead of NIST 3110 Ce solution, stable Ce isotope data were converted based on the normalization to BCR-2 measured in Bai et al., 2022[21] ($\delta^{142}Ce$ = 0.010±0.037‰). Therefore, BCR-2 value in Hu et al., 2023 is not included here.

Table S5 A compilation of radiogenic and stable Nd isotope values for reference materials analyzed in this study[a].

Sample Name	$^{143}Nd/^{144}Nd$	2SD	N[b]	$\delta^{145}Nd_{JNdi-1}$ (‰)	2SD	$\delta^{146}Nd_{JNdi-1}$ (‰)	2SD	$\delta^{148}Nd_{JNdi-1}$ (‰)	2SD	$\delta^{150}Nd_{JNdi-1}$ (‰)	2SD	N[c]	Reference
JNdi-1	0.512116	0.000008	29	-0.008	0.017	-0.005	0.010	-0.027	0.026	-0.027	0.029	3	**This study**
	0.512110					0.001	0.016	-0.005	0.045			12^{DS}	Liu et al., 2023b[19]
						0.001	0.031					89*	Bai et al., 2022a[21]
						0.000	0.030					50*	Bai et al., 2022b[18]
	0.512104	0.000008	6	0.000	0.029	0.000	0.027					210*	Bai et al., 2021[17]
				-0.006	0.031	-0.007	0.021					6*	Bai et al., 2021[17]
	0.512100	0.000008	39			0.003	0.017					39^{DS}	McCoy-West et al., 2017[15]
	0.512099	0.000005	61										Garcon et al., 2018[26]
	0.512093	0.000006	7										Roth et al., 2014[27]
	0.512112	0.000005	21										Rizo et al., 2011[28]
	0.512115	0.000007	133										Tanaka et al., 2000[29]
Ames I	0.512147	0.000012	12	0.051	0.010	0.109	0.011	0.203	0.012	0.308	0.011	3	**This study**
	0.512135	0.000014	9										Satkoski et al., 2017[30]
	0.512133	0.000018	8										Kylander-Clark et al., 2007[31]
	0.512146	0.000025	17										Lapen et al., 2005[32]
	0.512149	0.000022	24										Lapen et al., 2005[32]
	0.512143	0.000010	6										Beard et al., 1995[33]
Ames II	0.511974	0.000006	12	0.016	0.025	0.028	0.033	0.041	0.045	0.068	0.074	3	**This study**
	0.511968	0.000012	4										Satkoski et al., 2017[30]
	0.511964	0.000021	8										Kylander-Clark et al., 2007[31]
	0.511972	0.000016	28										Lapen et al., 2005[32]
	0.511975	0.000018	57										Lapen et al., 2005[32]
BCR-2	0.512636	0.000008	22	-0.018	0.007	-0.031	0.017	-0.071	0.026	-0.099	0.032	6	**This study**

	0.512625					-0.026		-0.061				1[DS]	Liu et al., 2023b[19]
						-0.024	0.033					7*	Bai et al., 2023[34]
						-0.048	0.028					3*	Bai et al., 2022a[21]
						-0.036						1*	Bai et al., 2022a[21]
						-0.020	0.031					3*	Bai et al., 2022b[18]
	0.512623	0.000004	2			-0.020	0.018					2[DS]	McCoy-West et al., 2017[15]
	0.512636		5	-0.023	0.023							5	Saji et al., 2016[13]
				-0.046	0.018	-0.074	0.016	-0.162	0.064			5	Ma et al., 2013[12]
	0.512635	0.000012	20									20	Wang et al., 2017[14]
	0.512638	0.000015	10										Weis et al., 2006[1]
	0.512634	0.000010	13										Li et al., 2012[35]
mean						***-0.035***	***0.034***						***interlaboratory***
BHVO-2	0.512989	0.000010	30	-0.009	0.020	-0.024	0.024	-0.052	0.045	-0.081	0.069	8	**This study**
	0.512979					-0.041		-0.057				1[DS]	Liu et al., 2023b[19]
						-0.054	0.044					1[DS]	Hu et al., 2023[d 22]
						-0.031	0.028					9*	Bai et al., 2023[34]
						-0.029	0.018					3*	Bai et al., 2022a[21]
						-0.031	0.033					3*	Bai et al., 2022b[18]
						-0.035						1*	Bai et al., 2022b[18]
	0.512987	0.000017	4	-0.008	0.031	-0.030	0.030					4*	Bai et al., 2021[17]
	0.512982	0.000010	17			-0.030	0.014					17[DS]	Mccoy-west et al., 2020[16]
	0.512985		5	-0.030	0.018							5	Saji et al., 2016[13]
				-0.059	0.024	-0.072	0.020	-0.172	0.082			5	Ma et al., 2013[12]
	0.512989	0.000012	20									20	Wang et al., 2017[14]
mean						***-0.038***	***0.028***						***interlaboratory***
COQ-1	0.512824	0.000012	4	-0.037	0.011	-0.074	0.042	-0.148	0.092	-0.225	0.167	2	**This study**
	0.512818	0.000003				-0.075	0.010	-0.129	0.022			2[DS]	Liu et al., 2023b[19]

	0.512800	0.000006	5										Erban Kochergina et al., 2022[36]
	0.512820	0.000006											Ackerman et al., 2017[37]
AGV-2	0.512793	0.000012	8	-0.008	0.008	-0.011	0.013	-0.031	0.014	-0.071	0.051	3	**This study**
	0.512784					-0.029		-0.049				1^{DS}	Liu et al., 2023b[19]
						-0.018	0.040					1^{DS}	Hu et al., 2023[22]
						-0.020	0.020					3*	Bai et al., 2022a[21]
						-0.039	0.024					3*	Bai et al., 2022b[18]
	0.512786	0.000010	4	0.004	0.04	-0.014	0.030					4*	Bai et al., 2021[17]
	0.512790	0.000018	20									20	Wang et al., 2017[14]
	0.512798	0.000008	6										Sanchez-Lorda et al., 2013[38]
	0.512793	0.000006	3										Cheong et al., 2013[39]
mean						***-0.022***	***0.019***						***interlaboratory***
GSP-2	0.511372	0.000010	9	-0.018	0.022	-0.029	0.044	-0.060	0.069	-0.116	0.133	3	**This study**
	0.511380					-0.044		-0.067				1^{DS}	Liu et al., 2023b[19]
						-0.038	0.034					5*	Bai et al., 2023[34]
						-0.038	0.024					3*	Bai et al., 2022a[21]
						-0.034	0.032					3*	Bai et al., 2022b[18]
	0.511361	0.000009	4	-0.028	0.028	-0.063	0.031					4*	Bai et al., 2021[17]
	0.511376		5	-0.020	0.005							5	Saji et al., 2016[13]
				-0.042	0.016	-0.071	0.018	-0.172	0.034			2	Ma et al., 2013[12]
	0.511389	0.000012											Chu et al., 2009[40]
	0.511374	0.000011	14										Weis et al., 2006[1]
mean						***-0.045***	***0.029***						***interlaboratory***
SDC-1	0.512071	0.000015	6	-0.015	0.001	-0.038	0.011	-0.088	0.043	-0.127	0.054	2	**This study**
	0.512062					-0.053		-0.085				1^{DS}	Liu et al., 2023b[19]
						-0.064	0.032					1^{DS}	Hu et al., 2023[22]
				-0.034	0.026	-0.071	0.020	-1.450	0.034			3	Ma et al., 2013[12]

	0.512040	0.000004	2										Li et al., 2011[41]
	0.512077	0.000026	3										Mahlen et al., 2008[42]
mean						***-0.057***	***0.025***						***interlaboratory***
JMn-1	0.512359	0.000008	8	0.007	0.005	0.010	0.015	0.024	0.012	0.002	0.014	2	**This study**
						0.000	0.05	-0.04	0.02				Ohno & Hirata, 2013[20]
NOD-A-1				0.001		0.032		0.039		0.074		1	**This study**
						0.043		0.079				1[DS]	Liu et al., 2023b[19]
						0.040		0.106				1[DS]	Liu et al., 2023b[19]
						0.080	0.022					1[DS]	Hu et al., 2023[22]
						0.013	0.032					3*	Bai et al., 2022a[21]
				-0.007	0.021	-0.015	0.028					4*	Bai et al., 2021[17]
mean						***0.032***	***0.058***						***interlaboratory***
NOD-P-1	0.512444	0.000014	3	-0.007		0.004		-0.046		-0.029		1	**This study**
	0.512427					0.000		-0.007				1[DS]	Liu et al., 2023b[19]
						0.016	0.038					1[DS]	Hu et al., 2023[22]
						0.024	0.029					3*	Bai et al., 2022a[21]
	0.512432	0.000014	4	-0.004	0.029	0.002	0.026					4*	Bai et al., 2021[17]
	0.512455	0.000095	68										Xu et al., 2018[43]
	0.512430	0.000015	6										Huang et al., 2012[44]
	0.512420	0.000011	5										Foster & Vance, 2006[45]
mean						***0.009***	***0.019***						***interlaboratory***

[a] Stable Nd isotope ($\delta^{142}Nd$) values are not reported in this study because ^{140}Ce was not monitored during our measurement to correct isobaric ^{142}Ce interferences. Stable isotope data in Wang et al., 2017[14] is not included because only $\delta^{142}Nd$ values were reported. Only a number of radiogenic $^{143}Nd/^{144}Nd$ data are compiled here, because it is a well-studied system that has been compiled in many previous publications. All published stable Nd isotope data are compiled here.

[b] N for radiogenic Nd isotope data is the total number of individual measurements combining repeated analyses in the same solutions and replicate analyses through independent purification in different batch runs.

[c] N for stable Nd isotope data is the number of independent replicate analyses through independent purification protocol for geological reference materials, each of which is comprised of at least 3 repeated measurements in the same solution; * indicates the number of sample-standard bracketing measurements for the same solution; ^{DS} indicates the double spike technique.

[d] Since Hu et al., 2023[22] used OL-REE as the bracketing standard instead of JNdi-1 Nd solution, stable Nd isotope data were converted based on the normalization to BCR-2 measured in Bai et al., 2022[21] ($\delta^{146}Nd$ = -0.048±0.028‰). Therefore, BCR-2 value in Hu et al., 2023 is not included here.

References

1. D. Weis, B. Kieffer, C. Maerschalk, J. Barling, J. de Jong, G. A. Williams, D. Hanano, W. Pretorius, N. Mattielli, J. S. Scoates, A. Goolaerts, R. M. Friedman and J. B. Mahoney, *GGG*, 2006, **7**, n/a-n/a.
2. R. Nakada, Y. Takahashi and M. Tanimizu, *Geochimica Et Cosmochimica Acta*, 2013, **103**, 49-62.
3. R. Nakada, Y. Takahashi and M. Tanimizu, *Geochimica Et Cosmochimica Acta*, 2016, **181**, 89-100.
4. R. Nakada, M. Tanaka, M. Tanimizu and Y. Takahashi, *Geochimica Et Cosmochimica Acta*, 2017, **218**, 273-290.
5. A. Laycock, B. Coles, K. Kreissig and M. Rehkämper, *JAAS*, 2016, **31**, 297-302.
6. R. Nakada, N. Asakura and K. Nagaishi, *GeocJ*, 2019, **53**, 293-304.
7. P. Bonnand, C. Israel, M. Boyet, R. Doucelance and D. Auclair, *JAAS*, 2019, **34**, 504-516.
8. H. Pourkhorsandi, V. Debaille, J. de Jong and R. M. G. Armytage, *Talanta*, 2021, **224**, 121877.
9. F. Liu, Z. Zhang, X. Li, Y. An, Y. Liu, K. Chen, Z. Bao and C. Li, *Anal Chem*, 2021, **93**, 12524-12531.
10. F. Liu, M. X. Ling, Z. F. Zhang, W. N. Lu, J. B. Xu, X. Li, D. Yang, J. J. Wu and H. Yang, *Chem Geol*, 2023, **637**, 121664.
11. S. Wakaki and T. Tanaka, *International Journal of Mass Spectrometry*, 2012, **323-324**, 45-54.
12. J. L. Ma, G. J. Wei, Y. Liu, Z. Y. Ren, Y. G. Xu and Y. H. Yang, *JAAS*, 2013, **28**, 1926.
13. N. S. Saji, D. Wielandt, C. Paton and M. Bizzarro, *JAAS*, 2016, **31**, 1490-1504.
14. Y. Q. Wang, X. X. Huang, Y. L. Sun, S. Q. Zhao and Y. H. Yue, *Analytical Methods*, 2017, **9**, 3531-3540.
15. A. J. McCoy-West, M. A. Millet and K. W. Burton, *Earth Planet Sci Lett*, 2017, **480**, 121-132.
16. A. J. McCoy-West, M. A. Millet, G. M. Nowell, O. Nebel and K. W. Burton, *JAAS*, 2020, **35**, 388-402.
17. J. H. Bai, F. Liu, Z. F. Zhang, J. L. Ma, L. Zhang, Y. F. Liu, S. X. Zhong and G. J. Wei, *JAAS*, 2021, **36**, 2695-2703.
18. J. H. Bai, J. L. Ma, G. J. Wei, L. Zhang, C. S. Liu, T. Gao, Y. H. Liu and Y. F. Liu, *Geostandards and Geoanalytical Research*, 2022, **46**, 825-836.
19. F. Liu, X. Li, H. Yang, Q. Y. Peng, J. J. Wu and Z. F. Zhang, *JAAS*, 2023, DOI: 10.1039/d3ja00284e.
20. T. Ohno and T. Hirata, *Anal Sci*, 2013, **29**, 47-53.
21. J. H. Bai, J. L. Ma, G. J. Wei, L. Zhang and S. X. Zhong, *JAAS*, 2022, **37**, 1618-1628.
22. J. Y. Hu, F. L. H. Tissot, R. Yokochi, T. J. Ireland, N. Dauphas and H. M. Williams, *ACS Earth and Space Chemistry*, 2023, **7**, 2222-2238.
23. J. Y. Hu, N. Dauphas, F. L. H. Tissot, R. Yokochi, T. J. Ireland, Z. Zhang, A. M. Davis, F. J. Ciesla, L. Grossman, B. L. A. Charlier, M. Roskosz, E. E. Alp, M. Y. Hu and J. Zhao, *Sci Adv*, 2021, **7**, eabc2962.
24. W. Li, X.-M. Liu, R. Nakada, Y. Takahashi, Y. Hu, M. Shakouri, Z. Zhang, T. Okumura and S. Yamada, *Earth Planet Sci Lett*, 2023, **602**, 117962.
25. W. S. Li, R. Nakada, Y. Takahashi, R. M. Gaschnig, Y. F. Hu, M. Shakouri, R. L. Rudnick and X. M. Liu, *Geochimica et Cosmochimica Acta*, 2023, **359**, 20-29.
26. M. Garçon, M. Boyet, R. W. Carlson, M. F. Horan, D. Auclair and T. D. Mock, *Chem Geol*, 2018, **476**, 493-514.
27. A. S. G. Roth, E. E. Scherer, C. Maden, K. Mezger and B. Bourdon, *Chem Geol*, 2014, **386**, 238-248.

28. H. Rizo, M. Boyet, J. Blichert-Toft and M. Rosing, *Earth Planet Sci Lett*, 2011, **312**, 267-279.
29. T. Tanaka, S. Togashi, H. Kamioka, H. Amakawa, H. Kagami, T. Hamamoto, M. Yuhara, Y. Orihashi, S. Yoneda, H. Shimizu, T. Kunimaru, K. Takahashi, T. Yanagi, T. Nakano, H. Fujimaki, R. Shinjo, Y. Asahara, M. Tanimizu and C. Dragusanu, *Chem Geol*, 2000, **168**, 279-281.
30. A. M. Satkoski, P. Fralick, B. L. Beard and C. M. Johnson, *Geochimica et Cosmochimica Acta*, 2017, **209**, 216-232.
31. A. R. C. Kylander-Clark, B. R. Hacker, C. M. Johnson, B. L. Beard, N. J. Mahlen and T. J. Lapen, *Chem Geol*, 2007, **242**, 137-154.
32. T. J. Lapen, L. G. Medaris, C. M. Johnson and B. L. Beard, *CoMP*, 2005, **150**, 131-145.
33. B. L. Beard, L. G. Medaris, C. M. Johnson, E. Jelinek, J. Tonika and L. R. Riciputi, *Geologische Rundschau*, 1995, **84**, 552-567.
34. J. H. Bai, K. Luo, C. Wu, Z. B. Wang, L. Zhang, S. Yan, S. X. Zhong, J. L. Ma and G. J. Wei, *Earth Planet Sci Lett*, 2023, **617**, 118260.
35. C. F. Li, X. H. Li, Q. L. Li, J. H. Guo, X. H. Li and Y. H. Yang, *Anal. Chim. Acta*, 2012, **727**, 54-60.
36. Y. V. Erban Kochergina, V. Erban and J. M. Hora, *Journal of Geosciences*, 2022, **67**, 273-285.
37. L. Ackerman, T. Magna, V. Rapprich, D. Upadhyay, O. Krátký, B. Čejková, V. Erban, Y. V. Kochergina and T. Hrstka, *Lithos*, 2017, **284-285**, 257-275.
38. M. E. Sánchez-Lorda, S. G. de Madinabeitia, C. Pin and J. I. G. Ibarguchi, *International Journal of Mass Spectrometry*, 2013, **333**, 34-43.
39. C. S. Cheong, J. S. Ryu and Y. J. Jeong, *Geosciences Journal*, 2013, **17**, 389-395.
40. Z. Chu, F. Chen, Y. Yang and J. Guo, *JAAS*, 2009, **24**, 1534.
41. C.-F. Li, X.-H. Li, Q.-L. Li, J.-H. Guo, X.-H. Li and T. Liu, *Anal. Chim. Acta*, 2011, **706**, 297-304.
42. N. J. Mahlen, B. L. Beard, C. M. Johnson and T. J. Lapen, *GGG*, 2008, **9**, n/a-n/a.
43. L. Xu, J. Yang, Q. Ni, Y. Yang, Z. Hu, Y. Liu, Y. Wu, T. Luo and S. Hu, *Geostandards and Geoanalytical Research*, 2018, **42**, 379-394.
44. K. F. Huang, J. Blusztajn, D. W. Oppo, W. B. Curry and B. Peucker-Ehrenbrink, *JAAS*, 2012, **27**, 1560.
45. G. L. Foster and D. Vance, *JAAS*, 2006, **21**, 288.